Journal of the Ceramic Society of Japan 116 [7] 777-780 2008 **Paper**

Potentiometric VOCs detection using 8YSZ based oxygen sensor

Masami MORI, Hiroyuki NISHIMURA, Hidenori YAHIRO and Yoshihiko SADAOKA†

Department of Materials Science and Biotechnology, Graduate School of Science and Engineering, Ehime University, 3, Bunkyo-cho, Matsuyama, Ehime 790−8577

Solid-state electrochemical sensors for volatile organic compounds (VOCs) based on commercial yttria stabilized zirconia (YSZ) sheet were fabricated using Pt or Pt covered with $SmFeO_3$ layers as electrodes. The sensing performances were strongly influenced by the surface morphology of YSZ. The overcoat with $SmFeO_3$ layer on the one side electrode enhanced the sensitivity for some VOCs. Even for 0.5 ppm of methyl ethyl ketone, ethanol and acetic acid, the changes of the electromotive force (EMF) in the levels of 20 mV and higher were confirmed at 400°C for the monolithic type sensor in which one side electrode was over-coated with $SmFeO_3$ powders.

Key-words : Zirconia, VOCs, EMF, Oxygen sensor, Gas sensor

[Received November 2, 2007; Accepted May 15, 2008]

1. Introduction

The air quality contamination by pollutant gases and volatile organic compounds (VOCs) has become a serious problem for human life. Thus, environmental monitoring is strongly demanded, especially in the urban spaces. Various techniques have been attempted to detect harmful gases. For the zirconia based oxygen sensor in potentiometric $P_a(O_2)$, Pt//YSZ// Pt, $P_c(O_2)$, the out put voltage (V) can be calculated from the thermodynamic relationship for reversible transfer of oxygen from cathode to anode according to Nernst's Eq. (1),

$$V = (RT/4F)\ln[P_c(O_2)/P_a(O_2)] \quad (1)$$

where R is the gas constant, T is absolute temperature, F is Faraday's constant, $P_a(O_2)$ and $P_c(O_2)$ are the oxygen concentration of anode and cathode electrodes, respectively. However, the output voltage value often deviates from the value estimated with Eq. (1), especially when a reducing gas coexists with oxygen. In 1977, Fleming interpreted this deviation as the non-Nernstian behavior resulting from the simultaneous presence of two electrochemical reactions occurring at the working electrode.[1)] Many research groups have found that the non-Nernstian behavior is based on the mixed potential of the working electrode. Among the various sensing devices, solid-state sensors are of practical interest due to their small size and ease of use. Zirconia-based electrochemical sensors tailored for NO_x, CO and hydrocarbons (HCs) detection have been widely investigated.[1)–11)]

In this work, to develop VOCs sensor based on the oxygen sensor with zirconia in a middle working temperature region of 350–450°C, the sensing characteristics in potentiometric were examined and the mechanism was discussed.

2. Experimental

2.1 Preparation of materials

The $SmFeO_3$ finer particles were prepared by the thermal decomposition of Sm-Fe-hexacyano complex.[12)] The heteronuclear complex, $Sm[Fe(CN)_6]\cdot 4H_2O$, was synthesized at room temperature by mixing aqueous solutions of equimolar amounts of $Sm(NO_3)_3$ and $K_3[Fe(CN)_6]$ under continuous stirring. The resulting precipitate was washed with water, ethanol and diethyl ether, before drying in air at 50°C. The complex was decomposed at 600°C for 24 h in flowing O_3/air, in order to obtain the perovskite-type powders. 0.24 g of the milled $SmFeO_3$ powder was dispersed in 30 ml of acetylacetone. The mixture was sonicated for 1 h at room temperature and left for 1 h. The smaller particle was obtained by the centrifugal separation of the supernatant liquid.

2.2 Fabrication of sensor device

The geometries of the sensor devices are illustrated in **Fig. 1**. 8YSZ sheet (8 mol% Y_2O_3/ZrO_2) of 200 μm in thickness from Tosoh Co. was used as the electrolyte. The Pt electrodes were prepared by the sputtering with a proper mask and heated at 600°C for 1 h. The thickness of the Pt electrodes was about 15 nm. Over-coating of the $SmFeO_3$ powders on the Pt electrode formed on the electrolyte was progressed with dc electrophoretic deposition technique (EPD) and then heat-treated in air. To prepare an organic suspension of the oxide particle for EPD, 0.24 g of $SmFeO_3$ was dispersed in 30 ml of acetylacetone and 7.5 mg of I_2 was added as a charging agent. The mixture was stirred and then ultrasonicated for 1 h at room temperature to obtain a good dispersion. EPD was demonstrated under the constant dc voltage of 15 V for 2 min. The $SmFeO_3$ films were heat-treated at 300°C for 1 h. . The thickness of the $SmFeO_3$ films was around 10 μm.

2.3 Measurement of sensing properties

Sensing experiments were carried out in a conventional gas-flow apparatus equipped with a controlled heating facility. The sensor devices were alternatively exposed to different gases with and without VOCs lower than 10 ppm. The contaminated test gases with VOCs, such as methyethylketone (MEK), acetic acid (AA), ethanol (EtOH) and benzene (Bz), were prepared with diffusion tubes. VOC concentration was controlled with changing the flow rate and the temperature of the tube. The potential difference between the two electrodes of the sensing device was measured with a digital electrometer (Advantest R8340) at different temperatures.

† Corresponding author: Y. Sadaoka; E-mail: sadaoka@eng.ehime-u.ac.jp

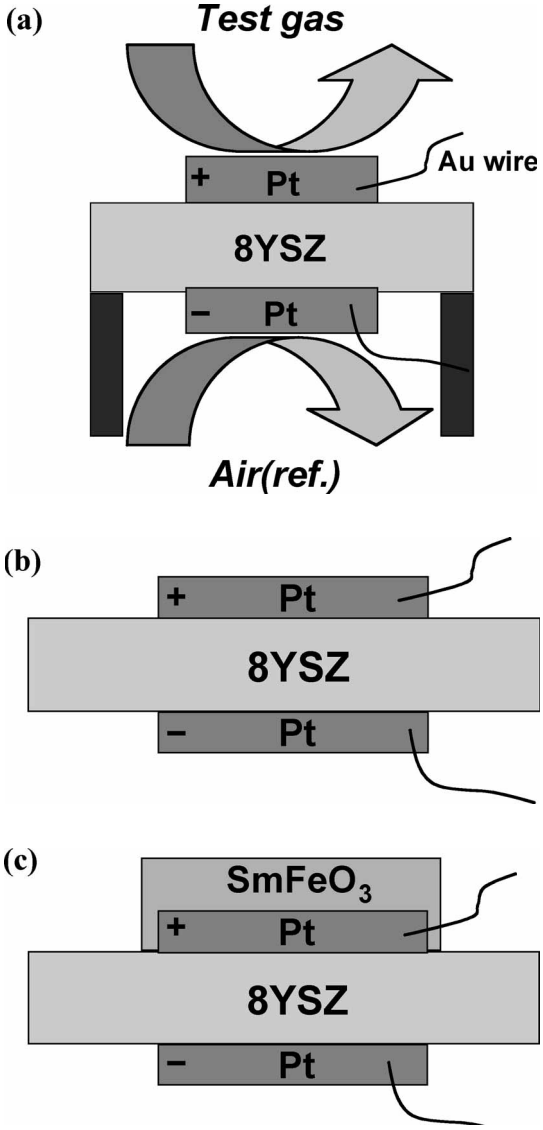

Fig. 1. Cross-sectional views of the YSZ-based devices, (a) Pt//8YSZ// Pt in separate-type, (b) Pt/8YSZ/Pt in monolithic-type, (c) $SmFeO_3$ coated Pt/8YSZ/Pt in monolithic-type.

3. Results and discussion

3.1 Fundamental response performance as an oxygen sensor in separate-type

The surfaces of the 8YSZ sheet used in this study were slightly different each other. The difference in gloss of the surfaces was easily detected. In the following discussions, the surfaces of the 8YSZ sheet are defined as *HG* and *LG* meaning high and low in gloss, respectively. The response behavior of the cells in a separate-type that the one side was exposed to the test gas with different concentrations of oxygen and the other side was exposed to a constant gas with 21% oxygen are shown in **Fig. 2**. The side exposed to the test gases was settled to (+) in polarity of the electrode. When the gas with the same concentration of oxygen with 21% was exposed to both sides, the out put voltage was almost zero. When pure nitrogen was exposed, the higher EMF was observed. For the device of that the *LG* side was exposed to the test gas and the *HG* side exposed a constant oxygen concentration of 21% (*LG*(+)), the EMF decreased with a decrease in the

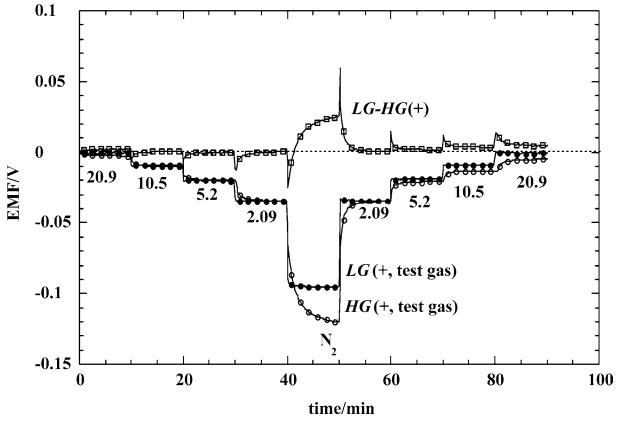

Fig. 2. EMF changes with oxygen concentration of the separate-type device Pt//8YSZ//Pt at 400°C. The side exposed to test gas and the O_2 concentration is indicated in the Fig. *LG-HG* means the difference of the V of *LG* and *HG*.

concentration of oxygen. For the device of that the *HG* side was exposed to the test gas (*HG*(+)), the change with changing concentration was more sluggish than that for the device of *LG*(+). The difference of the response observed for two types of devices is also shown in Fig. 2. The difference of the observed EMF in steady state was not so different in the range of 21–2%, excepting in pure nitrogen. In the nitrogen, the difference of the EMF was estimated to be 25 mV at 400°C. It is expected that the observed response difference between *LG*(+) and *HG*(+) was originated from the difference of the surface structure and/or morphology of 8YSZ. The kinetics of the reaction, $2O^{2-} \rightarrow O_2 + 4e^-$ at the electrode exposed to a lower oxygen concentration, was influenced by the physicochemical characteristics of the surface of 8YSZ.

The morphology of the surfaces of the YSZ-sheet used in this study was examined with SEM and XPS. The XPS results are summarized in **Fig. 3** and the observed SEM images are shown in **Fig. 4**. The surfaces of the sheet were slightly different in appearance, one-side was brilliant and the other-side was less brilliant (Fig. 4). For the used 8YSZ sheet, two signals of O1s were detected and the peaks appeared at 530 and 532 eV in binding energy were assigned to lattice and adsorbed oxygen ($O_{lattice}$ and O_{ad}), respectively. Before the sputtering of the surfaces in XPS chamber, the detected atomic ratios to Zr (*X*/Zr, *X* = O_{ad}, $O_{lattice}$, C, Y) of *HG* surface and *LG* surface were hardly different from each other (*HG*:●, *LG*:■ in Fig. 3). The sputtering of the

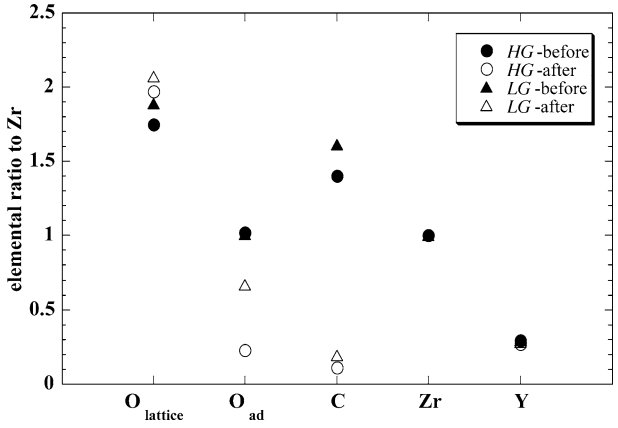

Fig. 3. XPS results of surfaces of 8YSZ sheet.

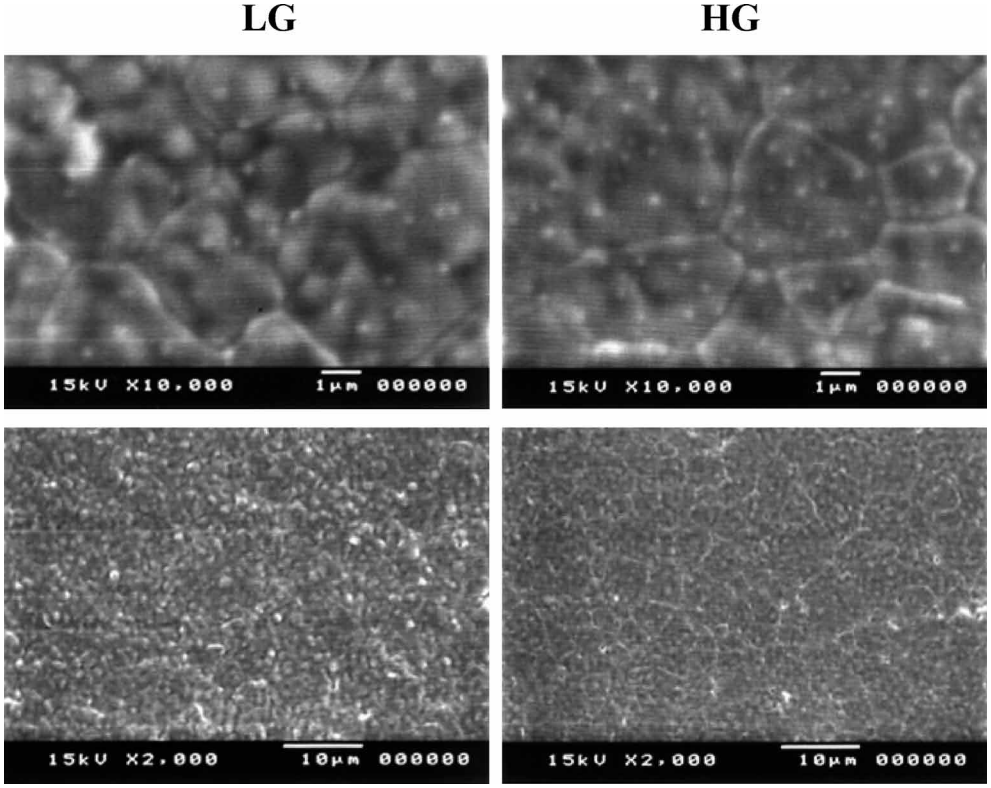

Fig. 4. SEM photograph of 8YSZ-sheet (surface). Surfaces of 8YSZ are slightly different in look, one side is brilliant (*HG*) and other side is less brilliant (*LG*).

surface resulted in a change of the concentration of the absorbed oxygen and carbonates to decrease. Even after the sputtering, the elemental ratios of *HG* surface and *LG* surface, Y/Zr, C/Zr and $O_{lattice}$/Zr were hardly different, but the O_{ad}/Zr was different. The O_{ad}/Zr for the *HG* surface was lower than that for the *LG* surface. The XPS results convinced us the difference of the response behavior between the half-cells.

3.2 Response for several VOCs of monolithic-type oxygen sensor

Monolithic-type device that both electrodes are exposed to the same gas environment is more practical device to detect various polluting gases.

Figure 5 shows response to AA of monolithic-type device Pt(*LG*,+)/8YSZ/Pt(*HG*,–) at 450°C. The EMF was clearly observed even when the same gas with AA was exposed to the both sides. The contamination of AA induced the increase in the voltage in plus rapidly and then slightly decreased to a steady state. The observed response is due to the difference of the response behavior between the two electrodes.

The response at 400°C to some other VOCs balanced with air from the cylinder was examined. The obtained calibration curves for VOCs are shown in **Fig. 6**. The response and its concentration dependency of VOCs were clearly observed. For the device that the *LG* surface was settled to plus (*LG*(+)), the EMF increased in positive. It is concluded that the activity of O^{2-} ion on the *HG* side was more decreased than the *LG* side by the contamination with the VOCs. The change of EMF enlarged with increasing

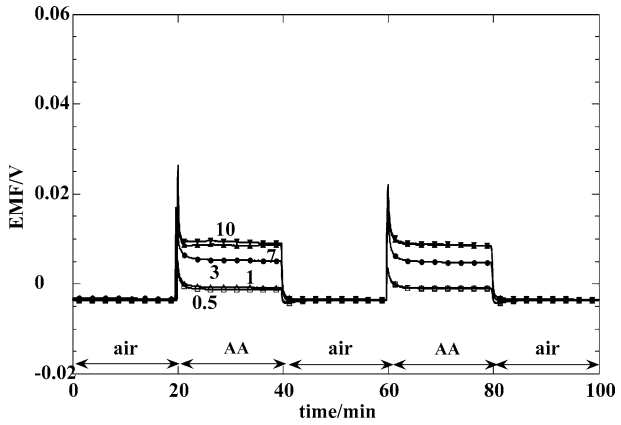

Fig. 5. Response to AA of the monolithic-type device Pt(*LG*,+)/8YSZ/Pt(*HG*,–) at 450°C. Concentration in ppm is indicated in the Fig.

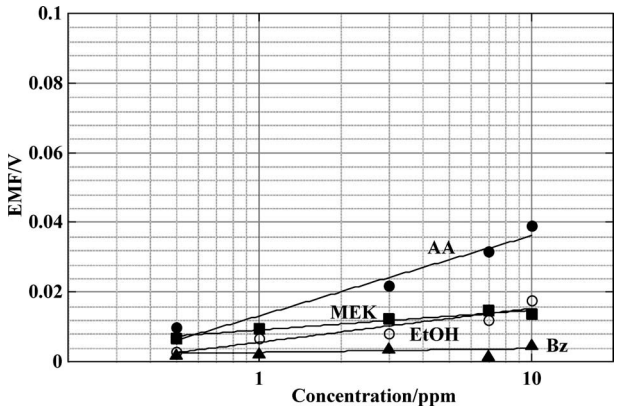

Fig. 6. EMF changes with the concentration of various VOCs of the monolithic-type device Pt(*LG*,+)/8YSZ/Pt(*HG*,–) at 400°C.

concentration of VOCs. It should be noticed that any regularities between the change of EMF and the concentration of Bz could not be observed and the change of EMF was very small. The observed lower response may be due to the low polarity of Bz.

3.3 Effects of the over-coating with $SmFeO_3$ layer on Pt electrode

To improve the response behavior of the device with Pt/8YSZ/Pt geometry, the coating of the Pt electrode with $SmFeO_3$ was considered. In several reports, a similar device with some perovskite-type oxides was examined.[2),6),11)] In these cases, the oxide layer was formed on the ionic electrolytes directly and the metal electrode was formed on the oxide. In our case, the metal electrodes were formed on YSZ directly and then the oxide layer was formed on to the Pt electrode of *LG* side. The lead was connected with metal electrodes in direct. The schematic illustration of examined device is shown in Fig. 1(c). The triple points formed on the YSZ interface and the oxide ($SmFeO_3$) layer was completely separated. **Figure 7** shows the response to AA balanced with air from the cylinder at 450°C. When the air without AA was exposed to the device, the observed EMF was almost zero.

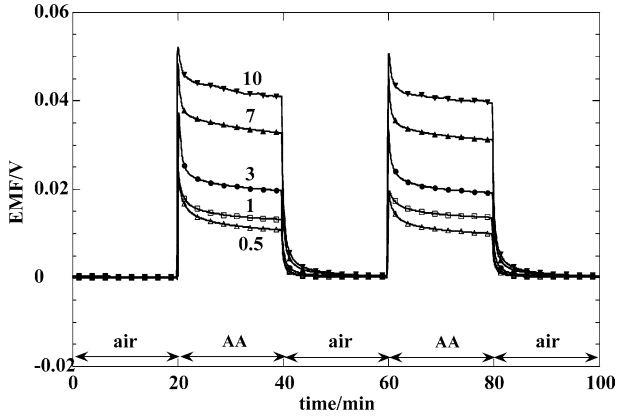

Fig. 7. Response to AA of the monolithic-type device $SmFeO_3$–Pt(*LG*,+)/8YSZ/Pt(*HG*,–) at 450°C. Concentration in ppm is indicated in the Fig.

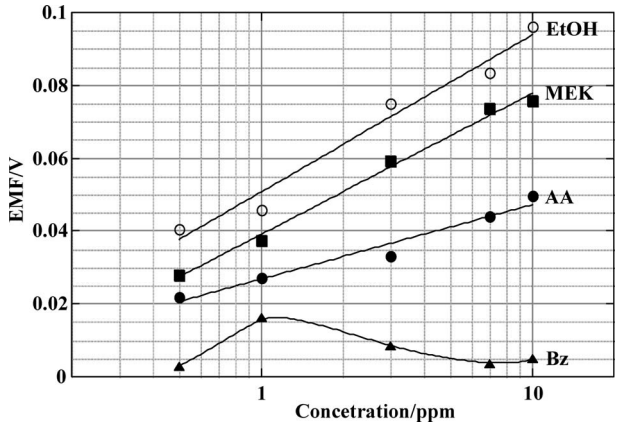

Fig. 8. EMF changes with the concentration of various VOCs of the monolithic-type device $SmFeO_3$–Pt(*LG*,+)/8YSZ/Pt(*HG*,–) at 400°C.

It is suggested that the activities of O^{2-} ion on the triple points on both side is almost same. The exposure to the air contaminated with AA resulted in an increase in the EMF in positive and then decreased gradually to a steady value. The EMF increased with an increase in the concentration of AA.

The response at 400°C to some other VOCs balanced with air from the cylinder was also examined. The obtained calibration curves at 400°C for VOCs are shown in **Fig. 8**. For MEK, EtOH and AA, the change of EMF enlarged with an increase in the concentration of VOCs. The over-coating with $SmFeO_3$ layer on to the one side of Pt electrode enhanced the sensitivity for some VOCs, expecting benzene. Higher sensitivity to VOCs observed for $SmFeO_3$, Pt(*LG*,+)/8YSZ/Pt(*HG*,–) geometry was originated from a less response to VOCs of the electrode over-coated with $SmFeO_3$ layer.

4. Conclusions

Solid-state electrochemical sensors for volatile organic compounds (VOCs) based on commercial YSZ sheet were fabricated using Pt and $SmFeO_3$ perovskite-type oxide as electrodes. The sensing performances were strongly influenced by the surface morphology of 8YSZ in the temperature range of 300–450°C. The over-coating with $SmFeO_3$ layer on the one side of Pt electrode enhanced the sensitivity for some VOCs excepting benzene. Even for 0.5 ppm of methyl ethyl ketone, ethanol, and acetic acid, the changes of the electromotive force in the levels of 20 mV and higher were confirmed at 400°C. The decrease in the activity of O^{2-} ion on the triple points due to VOCs contaminations was depressed by the over-coating of the Pt electrode with $SmFeO_3$ layer.

Acknowledgments This work was partly supported by CREST of Japan Science and Technology Agency.

References

1) W. Fleming, *Journal of the Electrochemical Society*, 124, 21–28 (1977).
2) N. F. Szabo and P. K. Dutta, *Solid State Ionics*, 171, 183–190 (2004).
3) E. L. Brosha, R. Mukundan, D. R. Brown and F. H. Garzon, *Sensors and Actuators*, B87, 47–57 (2002).
4) A. Vogel, G. Baier and V. Schüle, *Sensors and Actuators*, B15–16, 147–150 (1993).
5) G. Lu, N. Miura and N. Yamazoe, *Sensors and Actuators*, B35–36, 130–135 (1996).
6) N. Miura, T. Raisen, G. Lu and N. Yamazoe, *Sensors and Actuators*, B47, 84–91 (1998).
7) R. Sorita and T. Kawano, *Sensors and Actuators*, B40, 29–32 (1997).
8) T. Hibino, S. Kakimoto and M. Sano, *Journal of The Electrochemical Society*, 146 [9], 3361–3366 (1999).
9) T. Hibino, A. Hashimoto, S. Kakimoto and M. Sano, *Journal of The Electrochemical Society*, 148 [1], H1–H5 (2001).
10) N. Miura, M. Nakatou and S. Zhuiykov, *Ceramics and International*, 30, 1135–1139 (2004).
11) E. L. Broshu, R. Mukundam, D. R. Brown, F. H. Garzon, J. H. Visser, M. Zanini, Z. Zhou and E. M. Logothetis, *Sensors and Actuators*, B69, 171–182 (2000).
12) Y. Hosoya, Y. Itagaki, H. Aono and Y. Sadaoka, *Sensors and Actuators*, B108, 198–201 (2005).